

is interesting to note that the Fe catalyst produces a greater fraction of long chain hydrocarbon products ($C_{n>5}$) at higher pressures with 1/1 CO/H₂ feed. Comparison of the Fe and FeCo product distributions at 7.8 atmospheres (Figure 4.4.6) reveals that the alloy catalyst has the lesser ability to produce long chain products. In fact its product distributions with respect to hydrocarbon and methanol fractions is similar to that obtained with the 1/3 feed (Compare Figures 4.4.4 and 4.4.5 with 4.4.6 and 4.4.8). The methanol product fraction is relatively independent of feed suggesting that the methanol kinetics of this catalyst are less sensitive to feed composition compared to the Fe catalyst.

Figure 4.4.7 compare the product distribution of the alloy catalyst to that of pure Co at 7.8 atmospheres with the 1/1 feed. The greater fraction of long chain products for the Co catalyst indicates that the FeCo catalyst again has a much smaller tendency to incorporate CO into multicarbon products compared to the pure component catalyst. At total pressures of 14 atmospheres (Figure 4.4.8) the Fe catalyst further shifts its product distribution towards longer chain products while the principal shifts in the Fe Co catalyst is enhanced methanol and C₂ through C₄ paraffin.

4.4.2 Shifts in the Product Mole Fractions Due To Changing Pressure and Conversion Levels.

In the previous section, it is shown product mole fractions (P_i) exhibit a dependency on pressure and CO conversion levels. In order to clearly illustrate this point, product fractions at different pressures (constant CO conversion) and different CO conversions (constant pressure)

are made for each catalyst. Important product yield trends for each catalyst are then readily illustrated and direct comparisons can be made.

Figure 4.4.9 presents the product distributions for the Fe catalyst at both 1 and 14 atmospheres. There is only a marginal increase in the longer chain hydrocarbons while the principle shift with increasing pressure is the increase in PCH_3OH with a corresponding decrease in PCH_4 . At a fixed pressure an increase in the CO conversion level results in an increase in the produce mole fractions for the longer chain products (Figure 4.4.10 and 4.4.11). The product fraction of methanol decreases with increasing CO conversion suggesting the influence of secondary reactions unless the formation of higher molecular hydrocarbons inhibits the methanol production rate.

The Co catalyst typically exhibits decreased product fractions in the C_1 through C_4 olefins with increasing pressure while undergoing the largest increase in the C_5 and C_6^+ fractions compared to the other catalysts. These shifts are illustrated in Figures 4.4.12 and 4.4.13. Similar results are observed with increasing CO conversion levels at constant pressure (Figure 4.4.14).

Increasing pressure at a constant CO conversion level does not increase the long chain ($C_n > 5$) product fractions obtained with the alloy catalyst. In fact generally there is a decrease in the hydrocarbon product fractions with a corresponding large increase in the methanol fraction (Figures 4.4.15 and 4.4.16). At a constant pressure, increasing the CO conversion level results in marginal increases in long chain product fractions. Figure 4.4.17 shows the product distribution shift due to increasing conversion for the FeCo catalyst at 14 atmospheres using the 1/1 CO/H_2 feed. There is little change in the overall

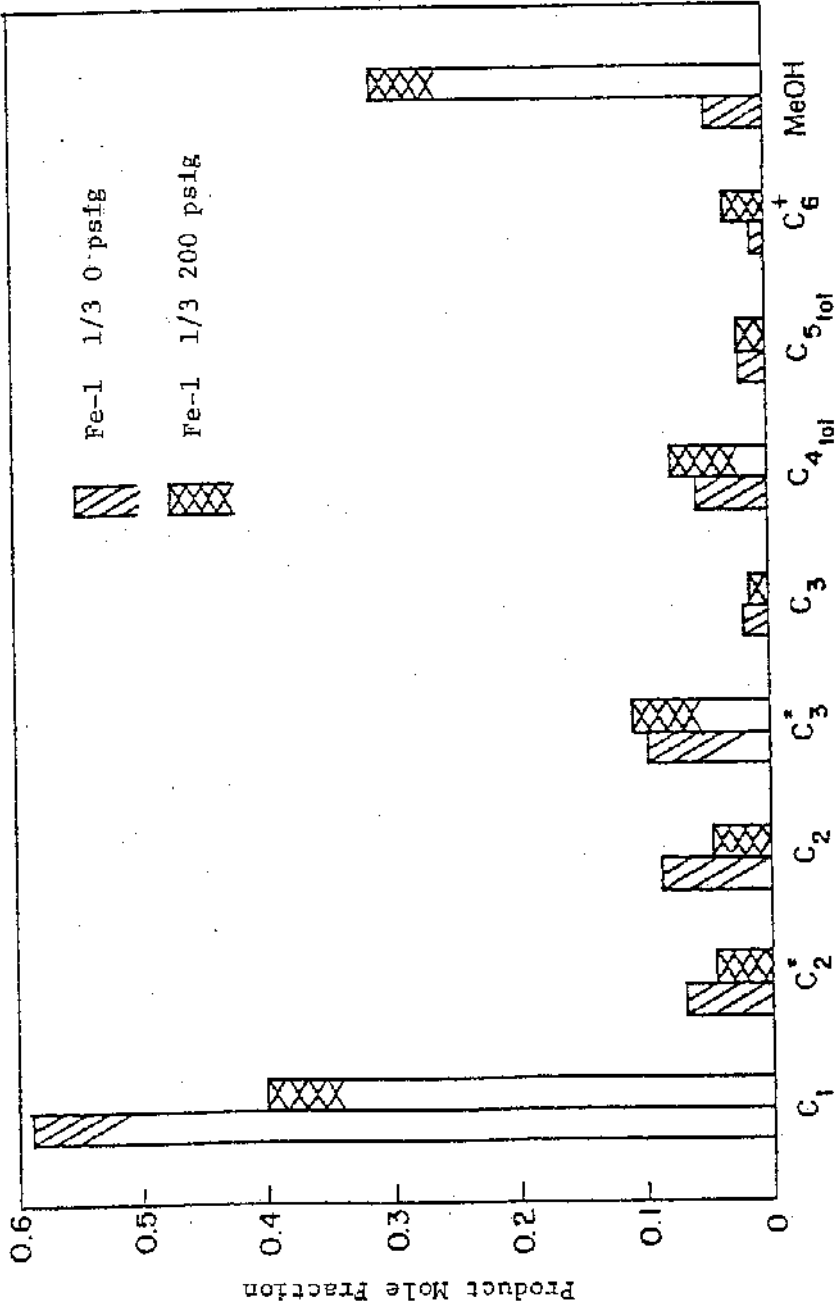


Figure 4.4.9 Effect of pressure on the product mole fraction of the Fe catalyst at 1.9% CO conversion 1/3 CO/H₂ feed, 250°C.

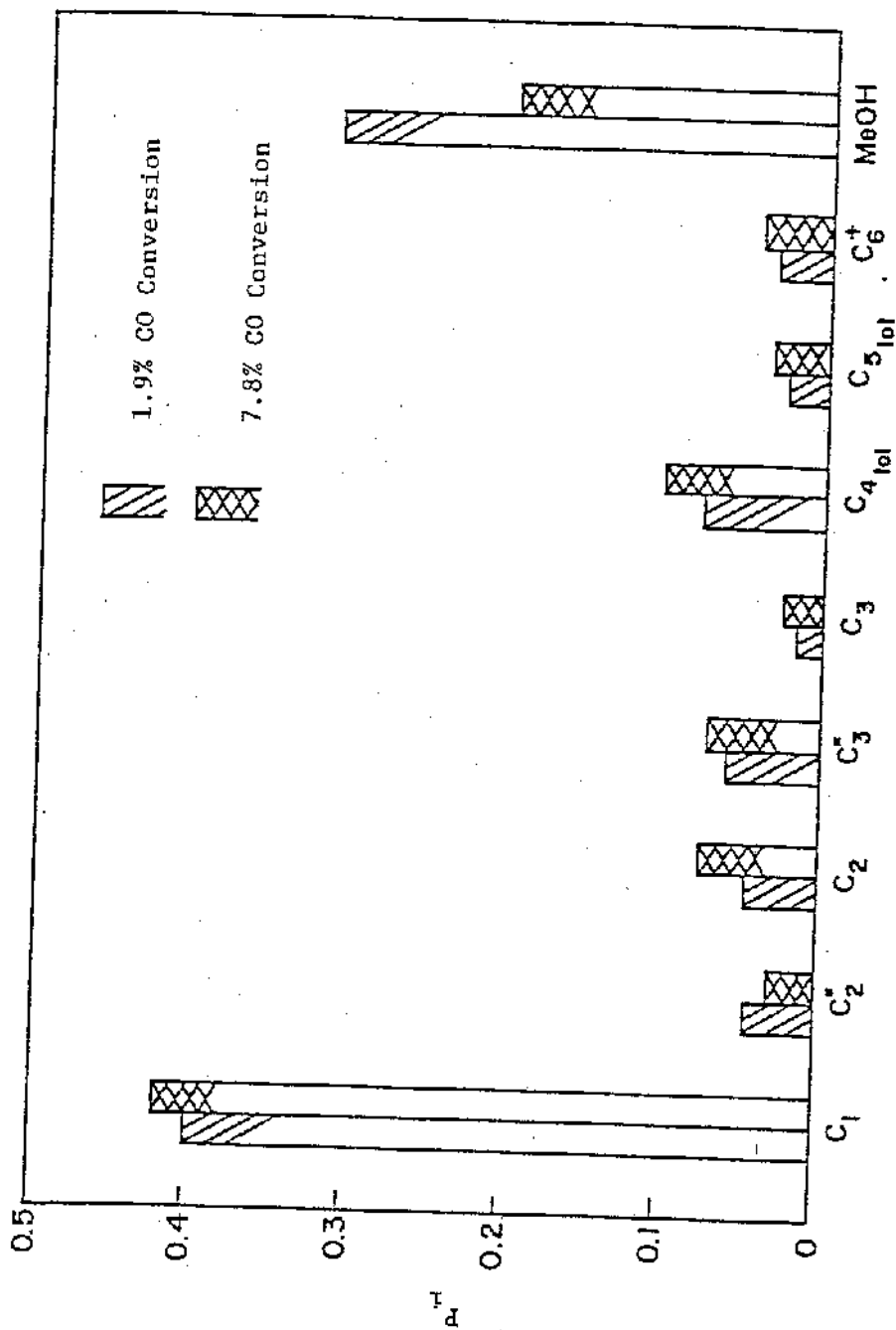


Figure 4.4.10 Product mole fractions for the Fe catalyst using the 1/3 CO/H₂ feed at 14 atm. and 250°C.

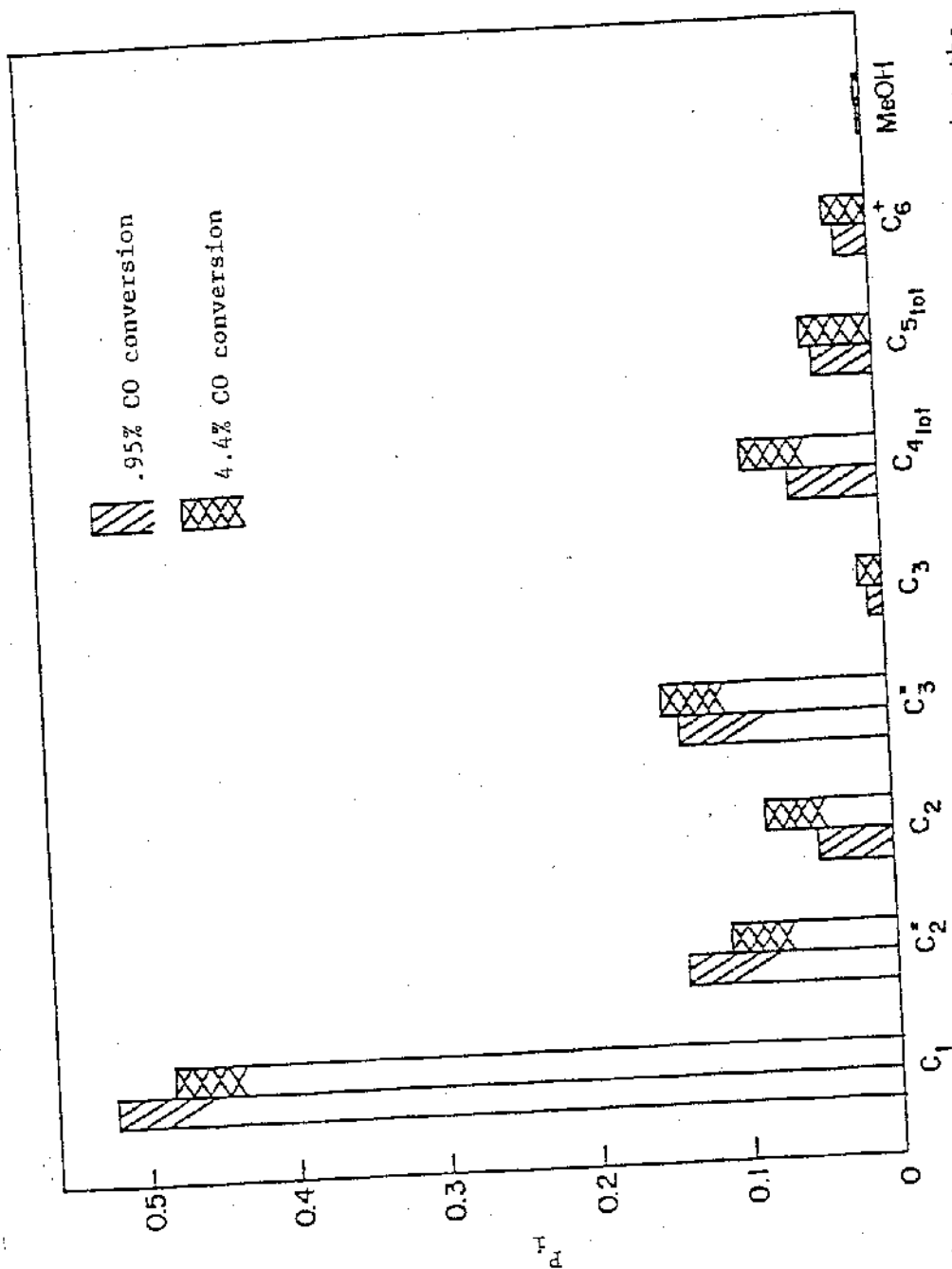


Figure 4.4.11 Product mole fractions for the Fe catalyst at 1 atm, using the 1/1 CO/H₂ feed at two different CO conversions.

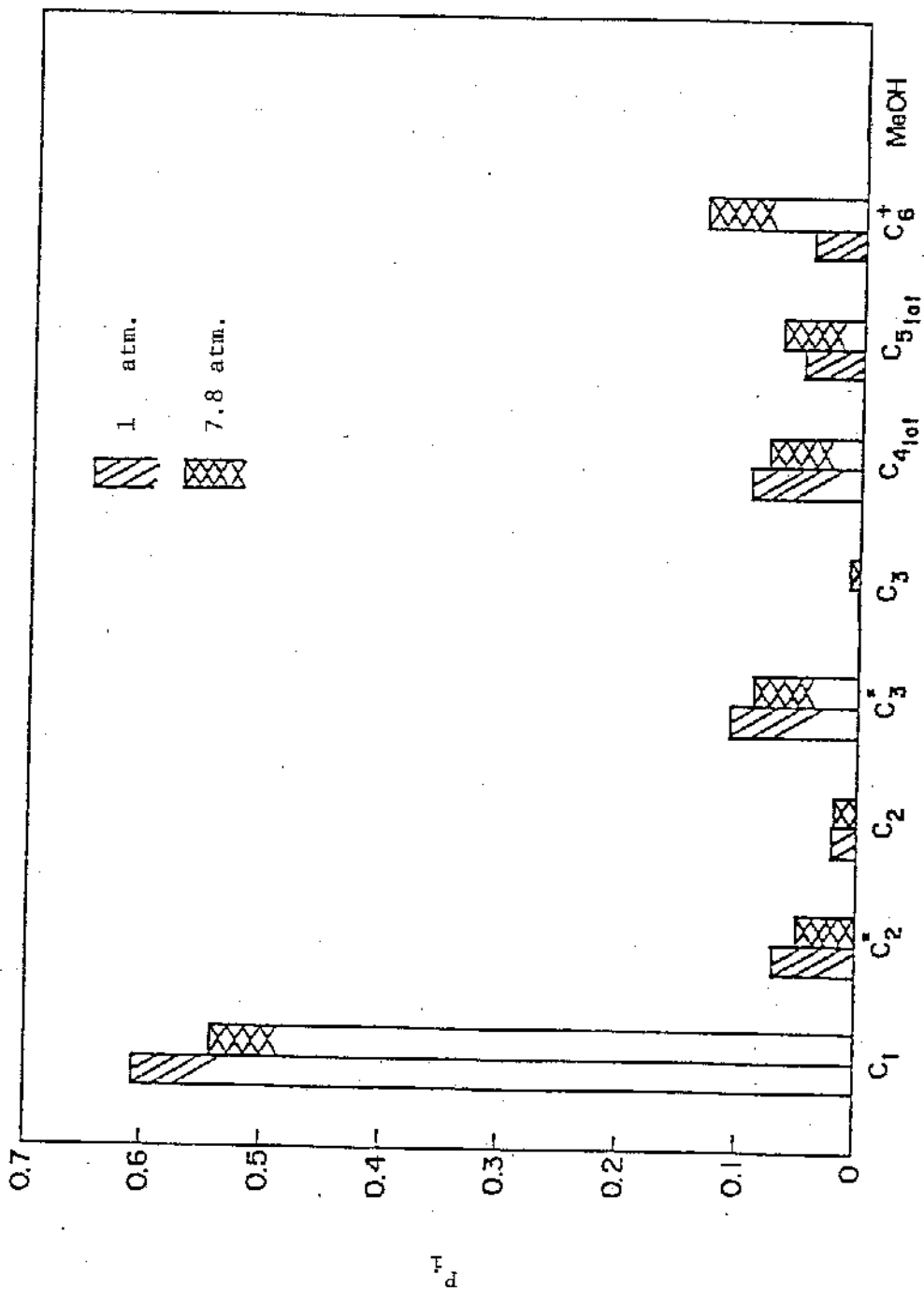


Figure 4.4.12 Product mole fractions for the Co catalyst using the 1/1 CO/H₂ feed at 250°C and a nominal CO conversion of 2%.

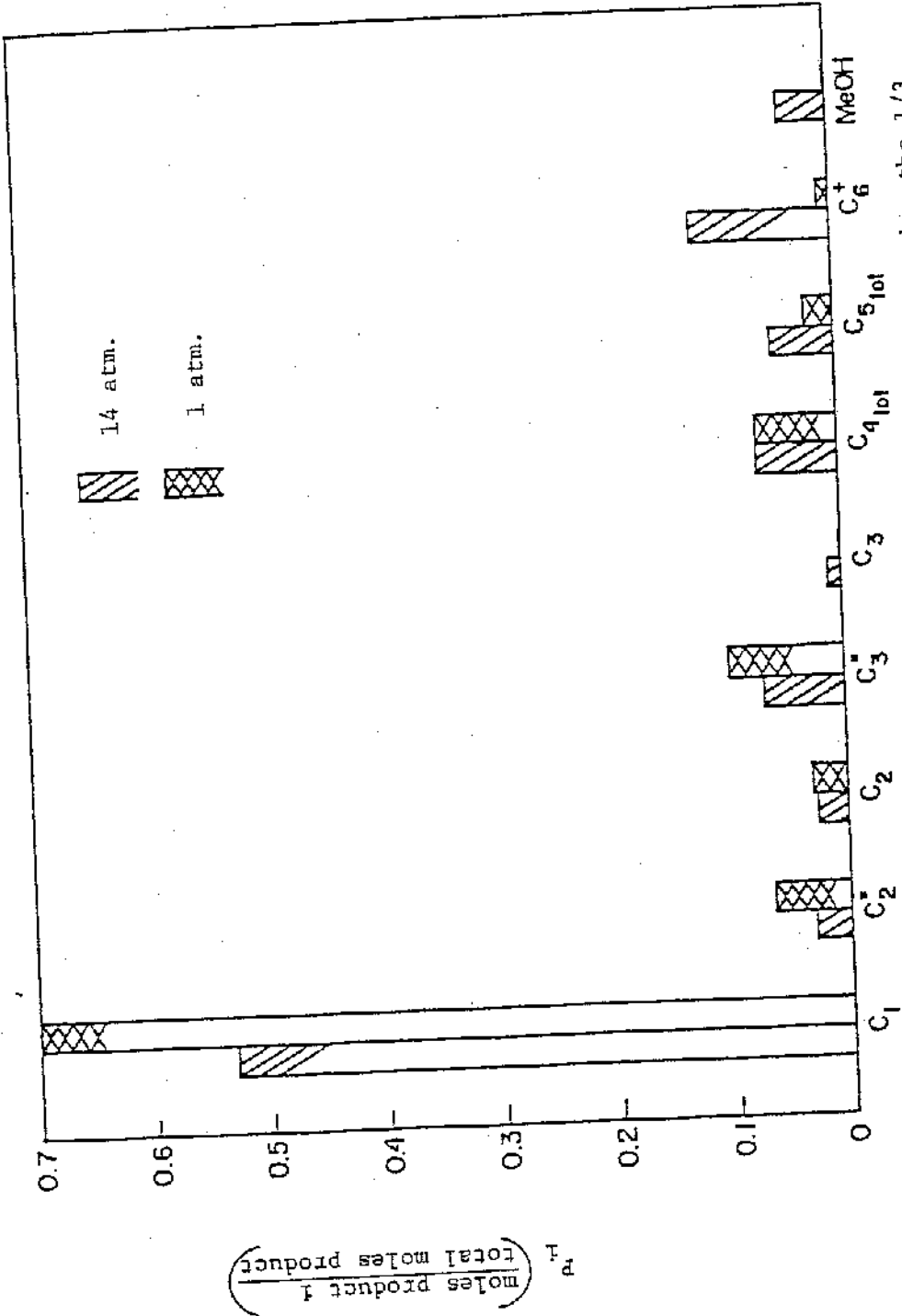


Figure 4.4.13 Product mole fractions for the Co catalyst using the 1/3 CO/H₂ feed at a nominal 1.8% CO conversion and 250°C.

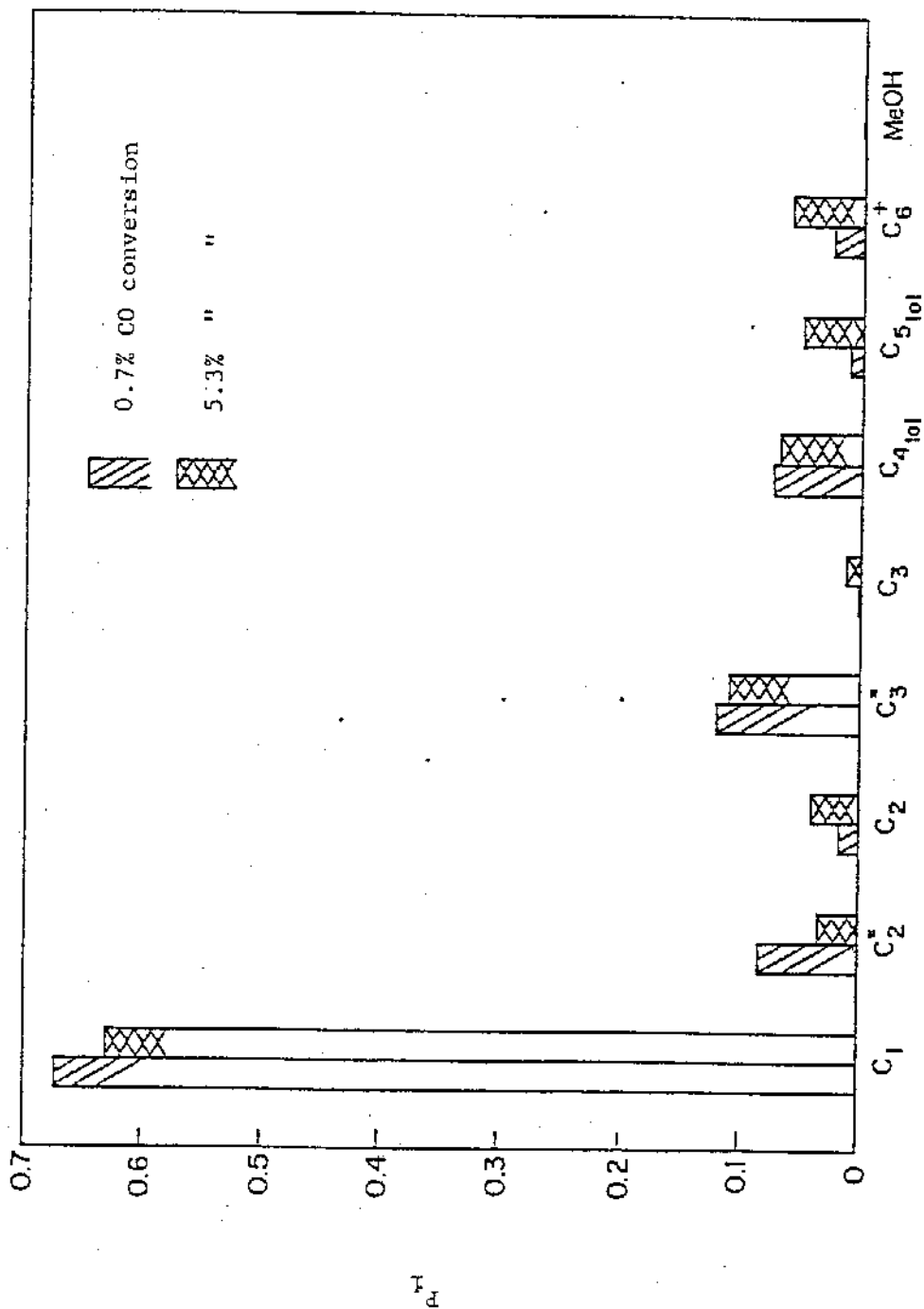


Figure 4.4.14 Product mole fractions for the CO conversion at two different CO conversions, 1 atm. and 250°C. 1/1 CO/H₂ feed.

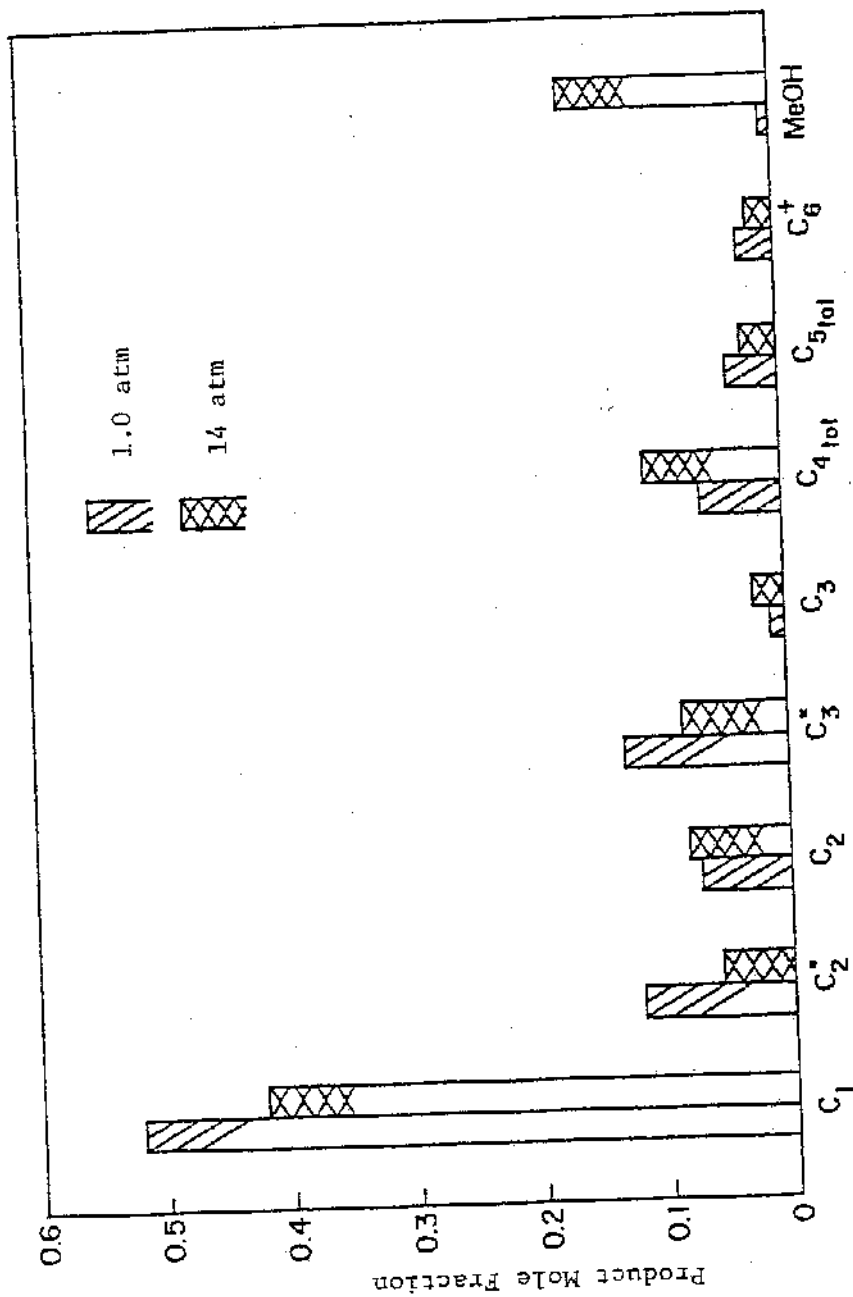


Figure 4.4.15 Effect of increasing pressure on the product mole fraction of the FeCo catalyst at 2.7% CO conversion 1/1 CO/H₂ feed, 250°C.

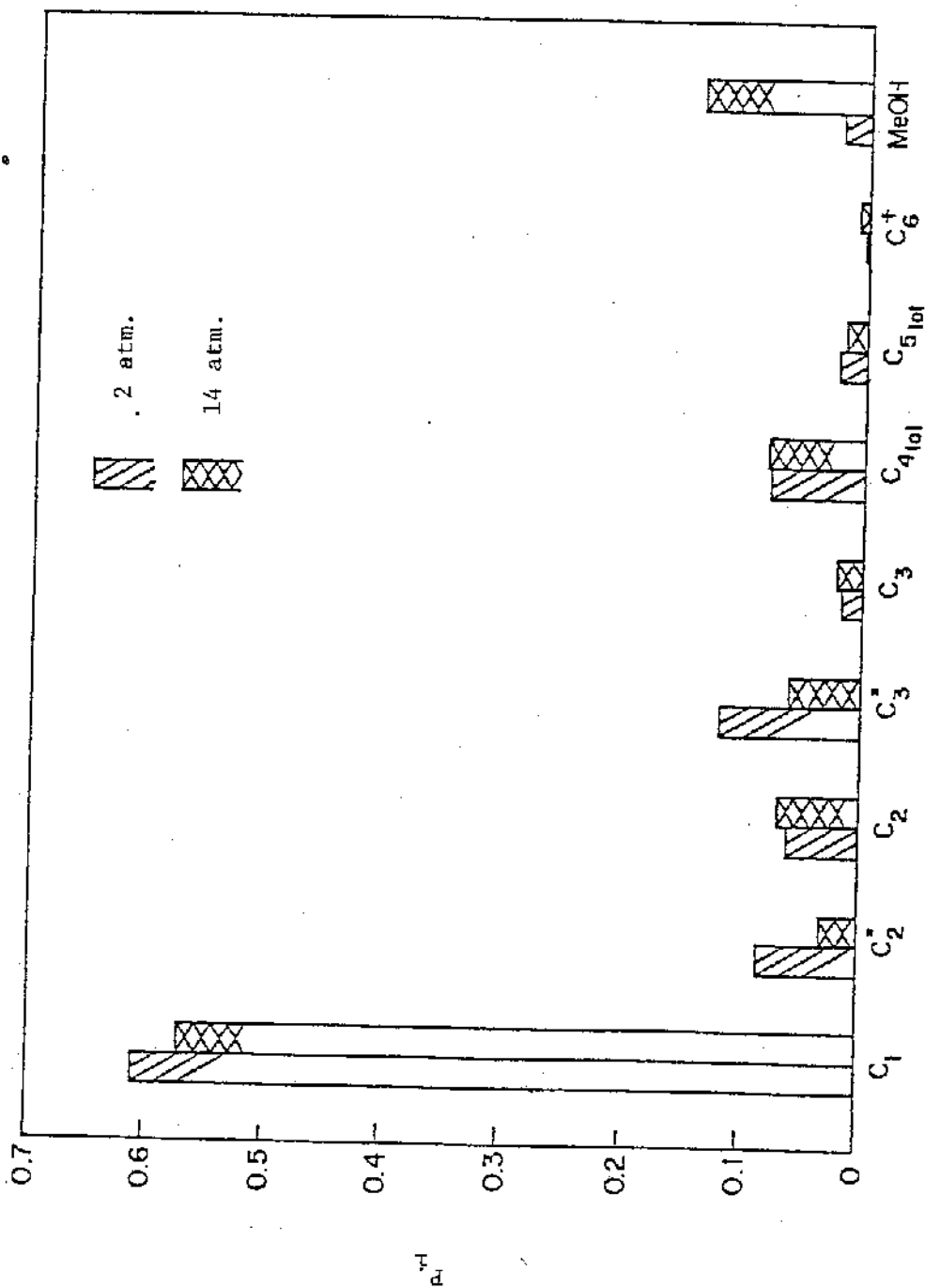


Figure 4.4.16 Product mole fractions for the FeCo catalyst at 1 and 14 atm. using the 1/3 CO/H₂ feed. The nominal CO conversion is 2.5%. Temperature = 250°C.

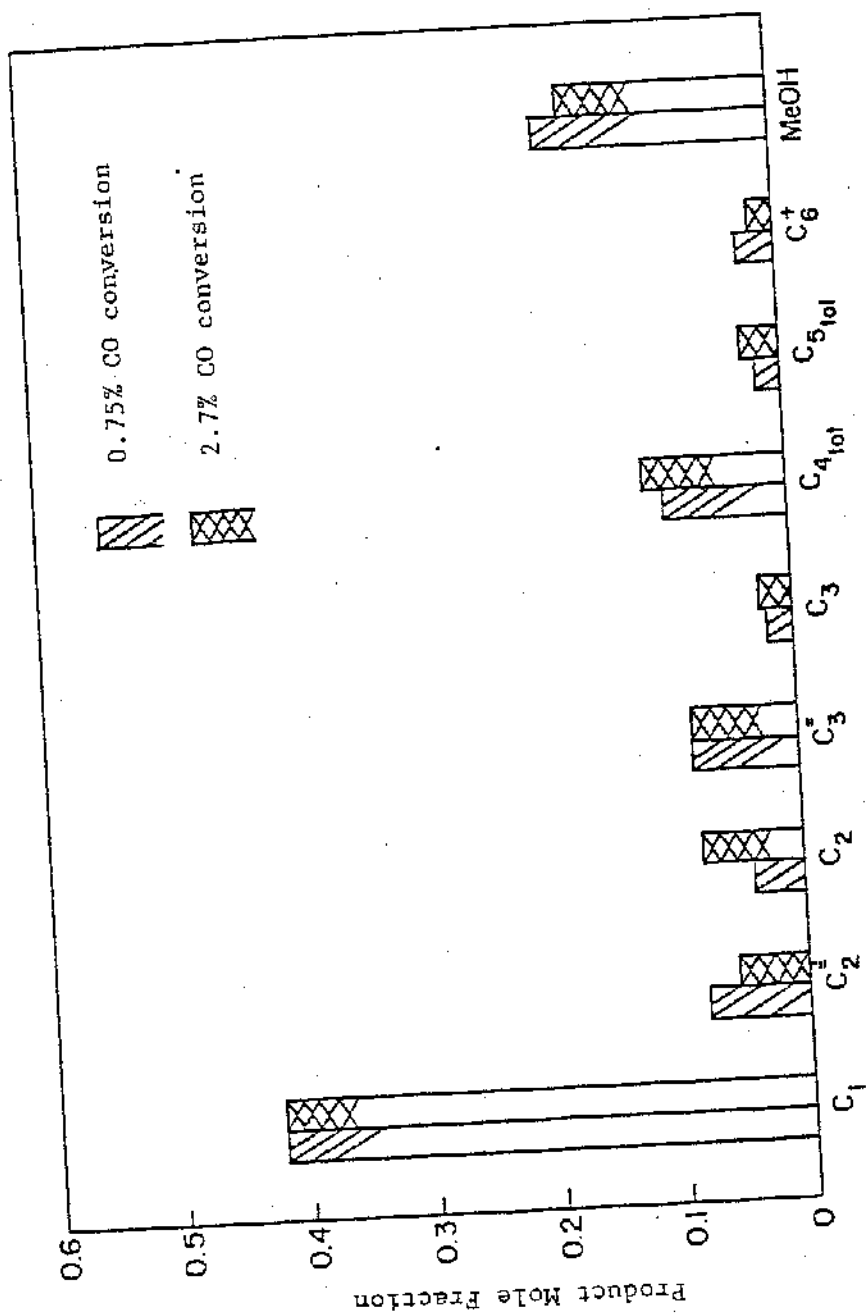


Figure 4.4.17 Effect of increasing CO conversion on the product mole fraction of the FeCo catalyst at 14 atm. 1/1 CO/H₂ feed, 250°C.

distribution other than an increase in the ethane fraction. Even a large increase in CO conversion results in only modest shifts in the distribution. Figure 4.4.18 presents steady state results obtained at 1.5% and 12% CO conversion. There are relatively small increases in the C_5 and C_6^+ product fractions compared to the increases observed for the Co (Figure 4.4.14) and Fe catalyst (4.4.10). It is also interesting to note that for the alloy catalyst the methanol fraction increases with increasing conversion while in the case for iron there is a decrease (Figure 4.4.10).

The product distribution's dependency on pressure and conversion level reflect the influence of product readsorption and secondary reactions on the overall synthesis process. The cobalt catalyst has the greatest ability to produce long chain products ($C_n > 5$) with increasing pressure and consequently the above mentioned factors (readsorption and secondary reaction) undoubtedly have the greatest effect on this catalyst. A weaker dependency exist in the case of the iron catalyst where the principle shift is the increase in methanol, at the conversion levels studied. However, it appears that methanol becomes less dominant a product with increasing conversion suggesting that either it is consumed via secondary insertion/chain initiation into hydrocarbon chains and/or its production is inhibited by readsorption of hydrocarbon products.

The alloy catalyst has the least ability to produce long chain products and indeed the effects of product readsorption and chain initiation are not readily observed for this catalyst. The greater relative hydrogenation activity of this catalyst (Section 4.3) may indeed be at least partially responsible for this behavior. Further comparisons

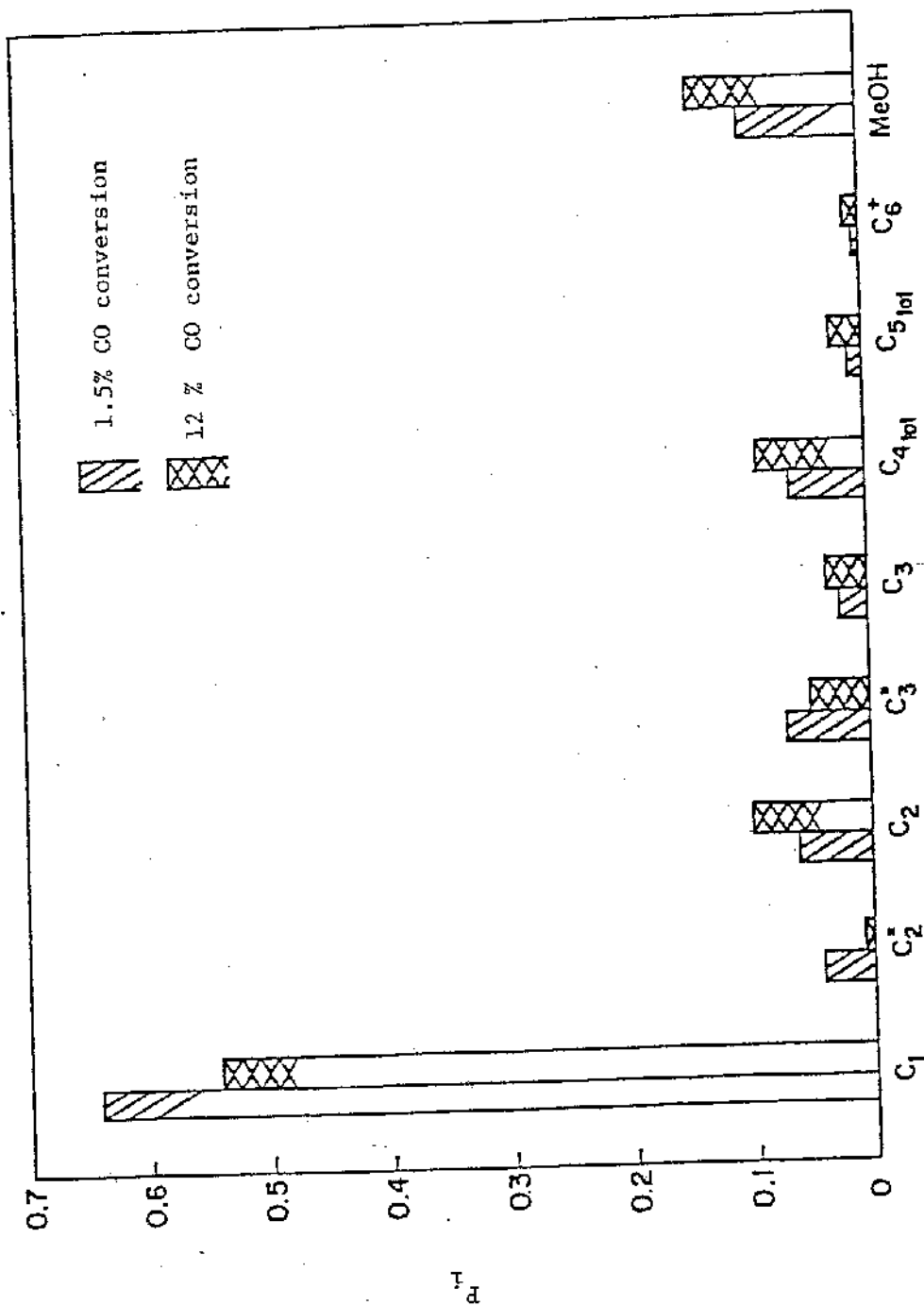


Figure 4.4.18 Product mole fractions for the FeCo catalyst using the 1/3 CO/H₂ feed at 14 atm. and 250°C.

are made in Sections 4.5, 5.3, and 5.4 for all three catalysts in which kinetic schemes are introduced in order to understand the hydrogenation and chain growth behavior as well as their dependency on feed pressure.

4.5.0 Schulz Flory Parameterization of Product Distribution

The steady state hydrocarbon product distributions (excluding methane) are presented in Figures 4.5.1 through 4.5.7 in terms of the Schulz Flory (SF) model discussed in Chapter 2. The equation used in obtaining the growth probability parameter, α , is shown below

$$\ln(Y_j \times 10^m) = n \ln(\alpha) + \phi_1 \quad 4.5.1$$

where Y_j is the product yield of component j

ϕ_1 is the y intercept

α is the probability of chain growth

$$\frac{r_{\text{propagation}}}{r_{\text{propagation}} + r_{\text{termination}}}$$

m is the scaling factor

The product yields are generally multiplied by 10^6 in equation 4.5.1 in order to shift the logarithm values to positive numbers. Table 4.5.1 provides a summary of the α values obtained for all catalysts and conditions studied.

Methane is not included in the SF analysis since its product yield does not generally correspond to SF kinetics. (56,6,91) Indeed the possibility exists that the reaction intermediates involved with methane production may be different than those responsible for the production of multicarbon products (87). In section 4.5.5 the product yields of the C_1 compounds (methane and methanol) are discussed.

Table 4.5.1 Schulz Flory Growth Probabilities

Catalyst Feed	Fe		Co		FeCo	
	1/3	1/1	1/3	1/1	1/1	1/1
<u>Pressure</u>						
1 atm	.432 (1.96) .419 (3.57)	.491 (2.7) .504 (3.6) .472 (.9) .370 (.9)	.467 (20) .44 (3.9)	.606 (2.0) .571 (3)	.329 (5.1)	.517 (1.9) .537 (2.9)
Average	<.425>	<.489>	<.464>	<.583>	<.468>	<.52>
7.8 atm.	.527 (3.1) .527 (2.)	.58 (4) .574 (2)	.763 (4.1) .786 (1.8) .754 (.8)	.817 (2) .875 (1)	.472 (6.8) .427 (3.7) .432 (1.1)	.477 (4.5) .491 (2.23) .474 (1.0)
Average	<.527>	<.577>	<.767>	<.856>	<.441>	<.48 >
14 atm.	.517 (1.8) .511 (7.8)	.576 (1.4) .564 (4)	.788 (2.5) .758 (3.5) .777 (7)	.817 (.8)	.367 (11) .367 (4.8) .357 (1.0) .364 (1.8)	.422 (3.68) .423 (1.54) .447 (.75) .437
Average	<.514>	<.57>	<.777>	<.817>	<.384>	<.437>

numbers in () % CO conversion

numbers in < > Average values